

Chapter 25

Strange and Non-strange Light-Flavour Hadron Production in Pb–Pb and p–Pb Collisions at LHC Energies with ALICE



Michal Šefčík

Abstract The ALICE experiment is dedicated to the study of strongly interacting matter at the extremely high temperatures and energy densities reached at the LHC. We report on the production of π , K and p measured with ALICE in p–Pb and Pb–Pb collisions at the top LHC energies of $\sqrt{s_{NN}} = 8.16$ and 5.02 TeV, respectively, as well as on the production of Λ , Ξ and Ω in Pb–Pb collisions at $\sqrt{s_{NN}} = 5.02$ TeV. Excellent tracking and particle-identification capabilities of the ALICE experiment allow characterising the hot nuclear matter via detailed measurements of particle production in nucleus-nucleus collisions. In addition, the study of proton-nucleus collisions provides a fundamental benchmark for initial state and cold nuclear matter effects.

25.1 Introduction

Measurement of light flavour hadron observables provides important information about the colliding system. In these proceedings we briefly discuss methods for particle reconstruction and identification with ALICE. Then we describe the study of the production of π , K and p in p–Pb collisions at $\sqrt{s_{NN}} = 8.16$ TeV and in Pb–Pb collisions at $\sqrt{s_{NN}} = 5.02$ TeV, as well as the study of the production of Λ , Ξ and Ω in Pb–Pb collisions at $\sqrt{s_{NN}} = 5.02$ TeV. The results include transverse momentum spectra ratios, Blast-Wave model fits, and yields integrated in transverse momentum as a function of multiplicity.

Michal Šefčík for the ALICE Collaboration.

M. Šefčík (✉)
Pavol Jozef Šafárik University, Košice, Slovakia
e-mail: michal.sefcik@cern.ch

25.2 Particle Detection in ALICE

The ALICE detector was designed for the study of heavy-ion collisions at the LHC. The main sub-detectors used to measure identified hadrons are the Inner Tracking System (ITS), the Time Projection Chamber (TPC), the Time-Of-Flight detector (TOF) and the High Momentum Particle Identification Detector (HMPID). The V0 detector is used for triggering and for the estimation of multiplicity and centrality. A full description of the ALICE sub-detectors can be found in [1, 2].

Charged light-flavour hadrons (π , K, p) are identified using combined information from ITS, TPC, TOF and HMPID detectors. Weakly decaying strange particles (K_S^0 , Λ , Ξ , Ω) are reconstructed via their characteristic decay topologies. For a detailed description, see similar analyses [3, 4].

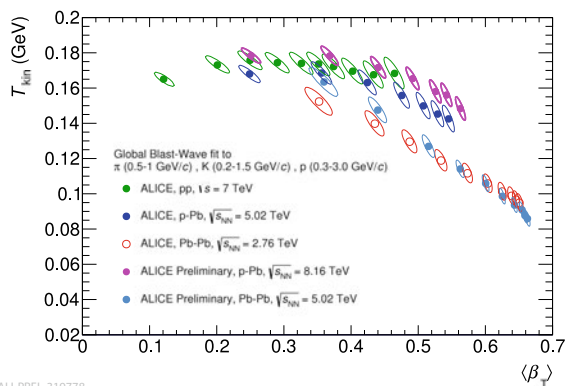
25.3 Results

The transverse momentum spectra of pions, kaons and protons have been fitted simultaneously with a Blast-Wave function [5]. The resulting fitted parameters are presented in Fig. 25.1. The evolution with multiplicity in Pb–Pb collisions at $\sqrt{s_{NN}} = 5.02$ TeV follows a trend similar to that observed at the lower energy $\sqrt{s_{NN}} = 2.76$ TeV, with further increase in radial expansion velocity. In p–Pb collisions at $\sqrt{s_{NN}} = 8.16$ TeV, we observe higher kinetic freeze-out temperature than at the lower energy $\sqrt{s_{NN}} = 5.02$ TeV.

The K/ π and p/ π ratios are shown in Fig. 25.2 for p–Pb collisions and in Fig. 25.3 for Pb–Pb collisions. The p/ π ratio exhibits a pronounced enhancement at intermediate p_T in central Pb–Pb collisions w.r.t. peripheral collisions. The K/ π ratio enhancement is comparatively negligible.

Figure 25.3 also shows a comparison of spectra ratios to hydrodynamic models. The models used are: iEBE-VISHNU hybrid model [6, 7], McGill [8] and

Fig. 25.1 Blast-wave parameters resulting from a simultaneous fit of π , K and p spectra. T_{kin} represents the kinetic freeze-out temperature and β_T the radial expansion velocity. The fit ranges are specified in the plot legend. Various collision systems and energies are shown



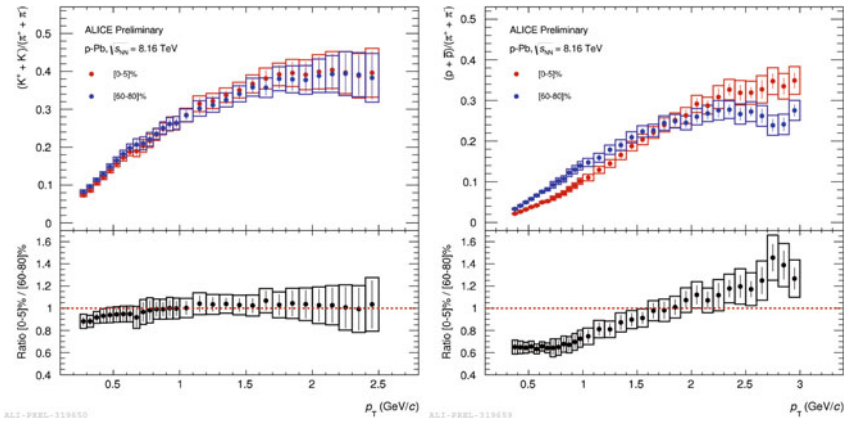


Fig. 25.2 $(K^+ + K^-)/(\pi^+ + \pi^-)$ (left) and $(p + \bar{p})/(\pi^+ + \pi^-)$ yield ratios as a function of transverse momentum in 0–5% and 80–90% centrality classes in p–Pb collisions at $\sqrt{s_{NN}} = 8.16$ TeV. In the lower part, the ratio of central to peripheral collisions is shown

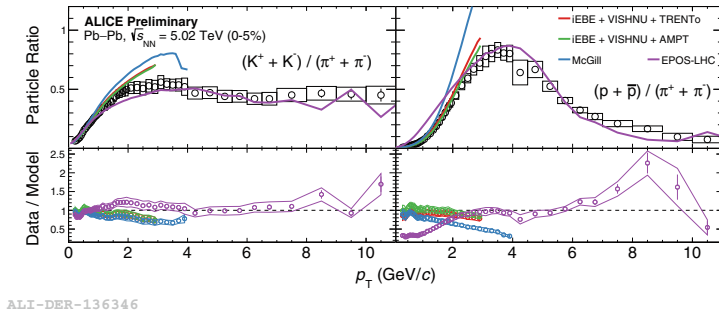


Fig. 25.3 $(K^+ + K^-)/(\pi^+ + \pi^-)$ (left) and $(p + \bar{p})/(\pi^+ + \pi^-)$ yield ratios as a function of transverse momentum in 0–5% centrality class in Pb–Pb collisions at $\sqrt{s_{NN}} = 5.02$ TeV. Comparison with hydrodynamic models is shown. In the lower part, the ratio of data to models is shown

EPOS [9]. All the hydrodynamic models describe the behaviour at low p_T . EPOS, which includes radial flow and jet-medium interactions, describes the dependence over the entire p_T range.

The p/π and Ω/π ratios of p_T -integrated yields are shown in Fig. 25.4 as a function of multiplicity. All measured collision systems and energies follow a common trend. The increase in small systems observed for strange particles is more pronounced for particles with greater strangeness content. For strange particles, there is a flat trend at high multiplicities. The p/π ratio exhibits a hint of decrease at high multiplicities.

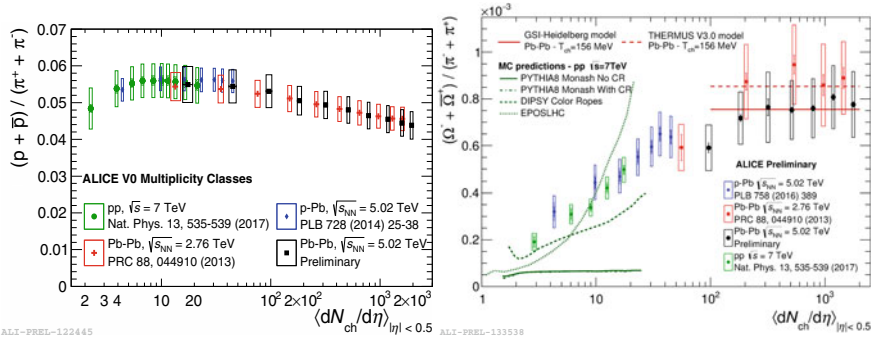


Fig. 25.4 Ratio of proton (left) and Ω (right) yields to pion yield as a function of charged particle multiplicity at medium pseudo-rapidity. Data from pp collisions at $\sqrt{s} = 7$ TeV, p–Pb collisions at $\sqrt{s_{NN}} = 5.02$ TeV and Pb–Pb collisions at $\sqrt{s_{NN}} = 2.76$ TeV and $\sqrt{s_{NN}} = 5.02$ TeV are shown

25.4 Conclusions

The production of light-flavour hadrons in p–Pb and Pb–Pb collisions was measured by ALICE. Blast-wave fits of the p_T spectra indicate that with the increase in energy, the radial expansion velocity increases in central Pb–Pb collisions and the kinetic freeze-out temperature increases in p–Pb collisions. The yield ratio to pions versus multiplicity has a continuous behaviour across colliding systems and energies.

References

1. K. Aamodt et al., (ALICE Collaboration): the ALICE experiment at the CERN LHC. *JINST* **3**, S08002 (2008)
2. B. Abelev et al., (ALICE Collaboration): performance of the ALICE experiment at the CERN LHC. *Int. J. Mod. Phys. A* **29**, 1430044 (2014)
3. B. Abelev et al., (ALICE Collaboration): multiplicity dependence of pion, kaon, proton and lambda production in p–Pb collisions at $\sqrt{s_{NN}} = 5.02$ TeV. *Phys. Lett. B* **728**, 25–38 (2014)
4. B. Abelev et al., (ALICE Collaboration): multi-strange baryon production at mid-rapidity in Pb–Pb collisions at $\sqrt{s_{NN}} = 2.76$ TeV. *Phys. Lett. B* **728**, 216–227 (2014)
5. E. Schnedermann, J. Sollfrank, U.W. Heinz, Thermal phenomenology of hadrons from 200 A/GeV S+S collisions. *Phys. Rev. C* **48**, 2462–2475 (1993)
6. C. Shen, Z. Qiu, H. Song, J. Bernhard, S. Bass, U. Heinz, The iEBE-VISHNU code package for relativistic heavy-ion collisions. *Comput. Phys. Commun.* **199**, 61–85 (2016)
7. W. Zhao, H.-J. Xu, H. Song, Collective flow in 2.76 A TeV and 5.02 A TeV Pb + Pb collisions. *Eur. Phys. J. C* **77**(9), 645 (2017)
8. S. McDonald, C. Shen, F. Fillion-Gourdeau, S. Jeon, C. Gale, Hydrodynamic predictions for Pb + Pb collisions at 5.02 TeV. *Phys. Rev. C* **95**(6), 064913 (2017)
9. K. Werner, B. Guiot, I. Karpenko, T. Pierog, Analysing radial flow features in p–Pb and p–p collisions at several TeV by studying identified particle production in EPOS3. *Phys. Rev. C* **89**(6), 064903 (2014)